

Supplementary Information for
Prediction of the two-dimensional ferromagnetic semiconductor
Janus 2H-ZrTeI monolayer with large valley and piezoelectric
polarizations

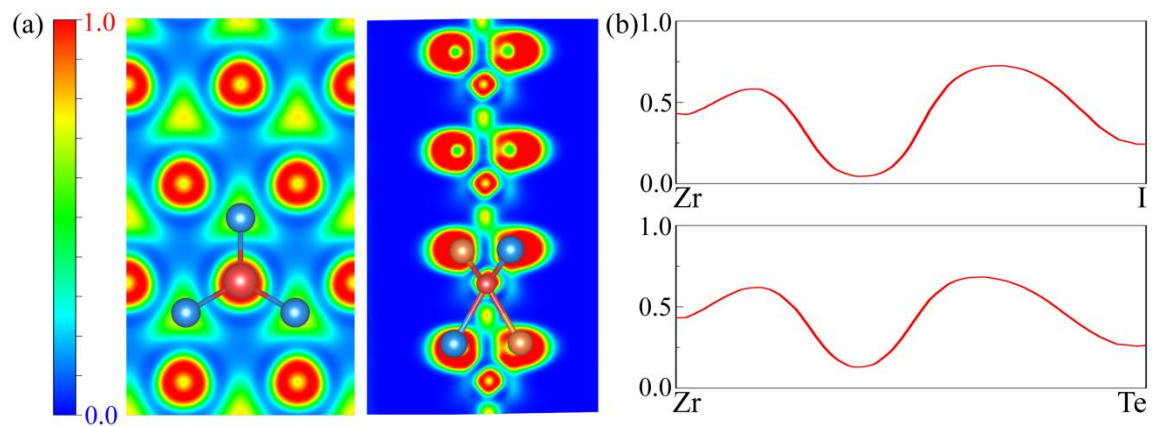


Fig. S1. (a) ELFs on the (001) and (110) planes. (b) ELF profiles along the paths Zr-I and Zr-Te.

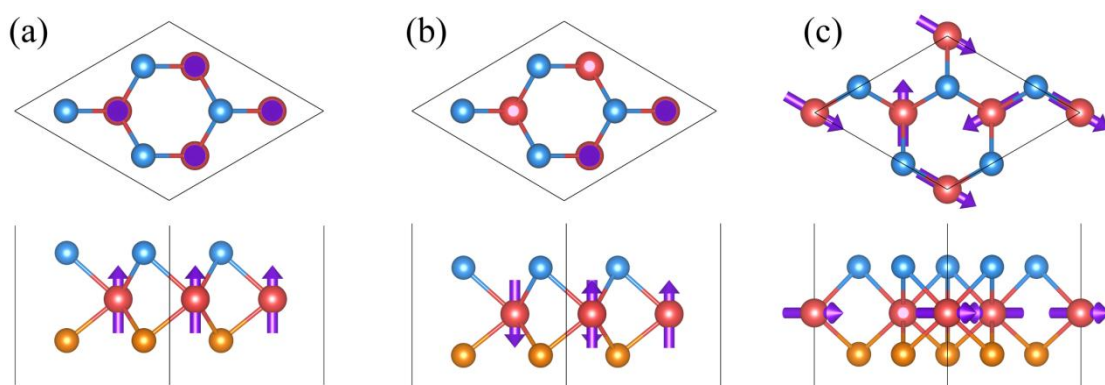


Fig. S2. Top and side views of the FM, collinear AFM and noncollinear 120°-Néel AFM states of the Janus ZrTeI monolayer.

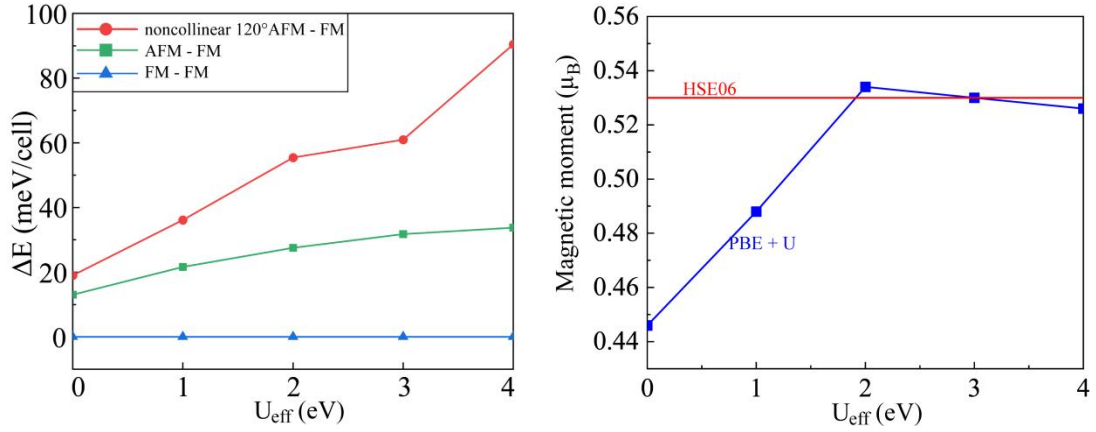


Fig. S3. Magnetic exchange energies of the collinear AFM and noncollinear 120°-Néel AFM states with respect to the FM state at different U_{eff} values. (b) Magnetic moments per formula unit of ZrTeI monolayer at different U_{eff} values.

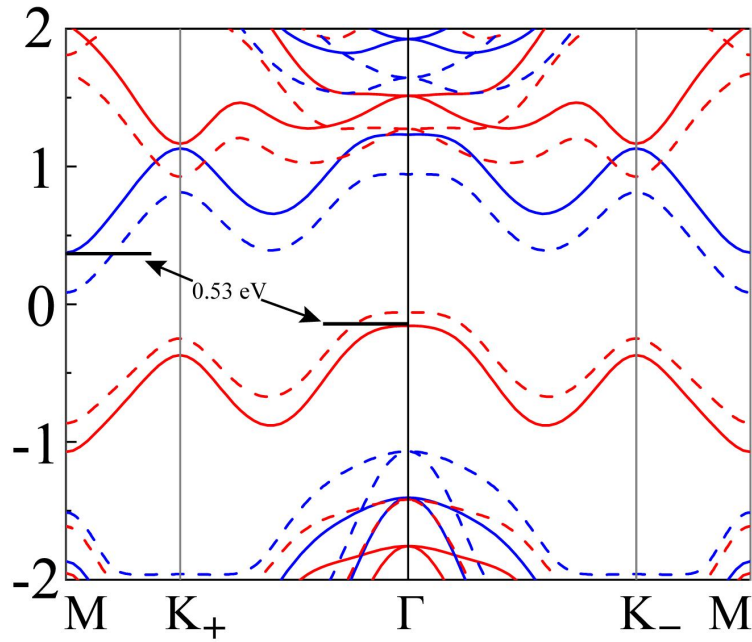


Fig. S4. Comparison of spin-resolved band structures calculated using the HSE06 method and the PBE + U method ($U_{\text{eff}} = 3$ eV), without considering the spin-orbit coupling effect. Solid lines represent the HSE06 method, dashed lines represent the PBE + U method, with red and blue lines indicating spin-up and spin-down, respectively.

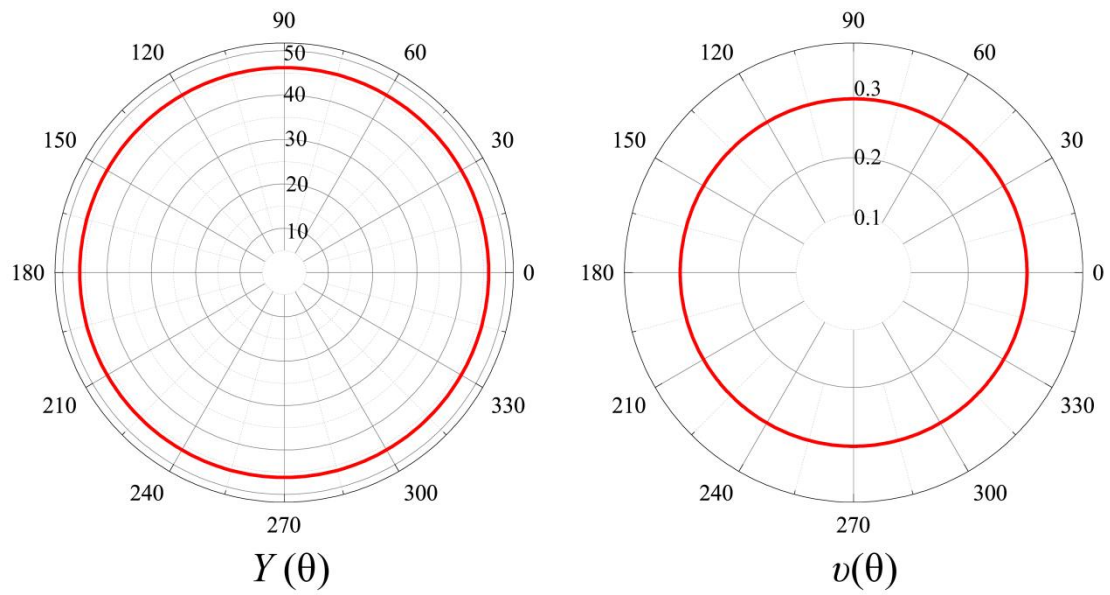


Fig. S5. Young's modulus $Y(\theta)$ and the Poisson's ratio $\nu(\theta)$ as a function of the in-plane angle θ for the ZrTeI monolayer.

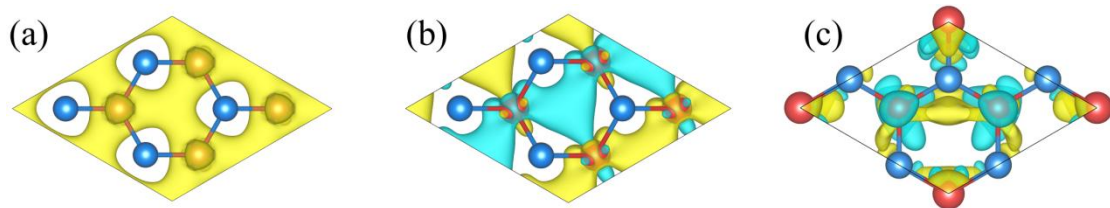


Fig. S6. Spin density distributions for different magnetic configurations are plotted, with yellow and cyan indicating spin-up and spin-down densities, respectively.

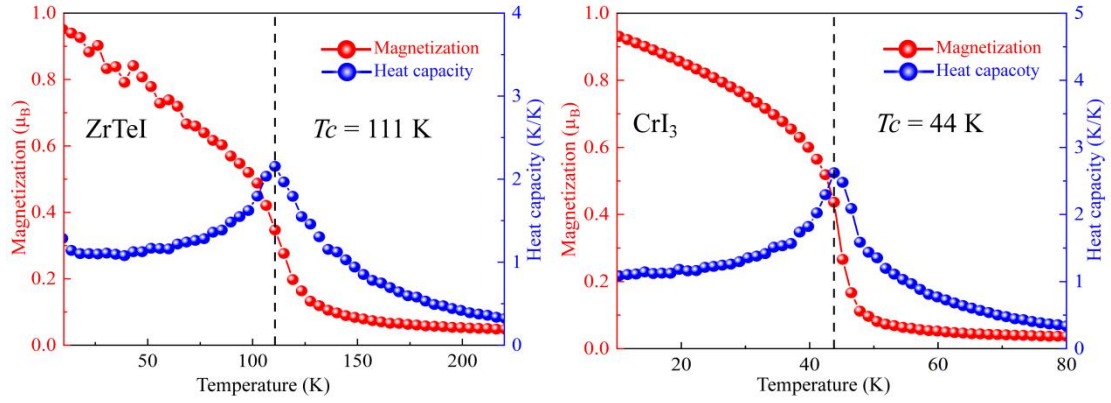


Fig. S7. (a) and (b) Temperature dependence of the normalized magnetization and specific heat capacity in Monte Carlo simulations of ZrTeI and CrI₃ monolayers.

The method for obtaining the magnetic interaction coefficients of the anisotropic Heisenberg model Hamiltonian through first-principles calculations is as follows. We consider four magnetic configurations in a $2 \times 2 \times 1$ supercell, with spins oriented along the x and z directions for both FM and AFM states. The corresponding energy expressions are:

$$E_{FM}^z = E_0 - (12J + 12\lambda + 4A)S^2 \quad (1)$$

$$E_{AFM}^z = E_0 + (4J + 4\lambda - 4A)S^2 \quad (2)$$

$$E_{FM}^x = E_0 - 12JS^2 \quad (3)$$

$$E_{AFM}^x = E_0 + 4JS^2 \quad (4)$$

Here, $|S|=1$, E_0 is the reference energy, and E_z and E_x are the energies calculated using the PBE + U + SOC method. Through simple algebraic operations, we obtain the values of J , λ , and A as 8.14 meV, -0.39 meV, and 0.0009 meV, respectively.

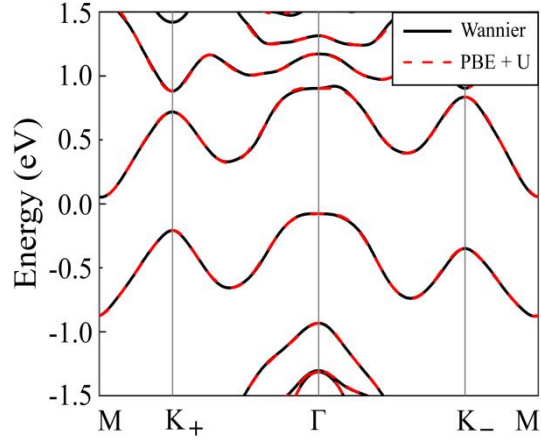


Fig. S8. Comparison of ZrTeI monolayer SOC band structures obtained with PBE + U and Wannier fitting.

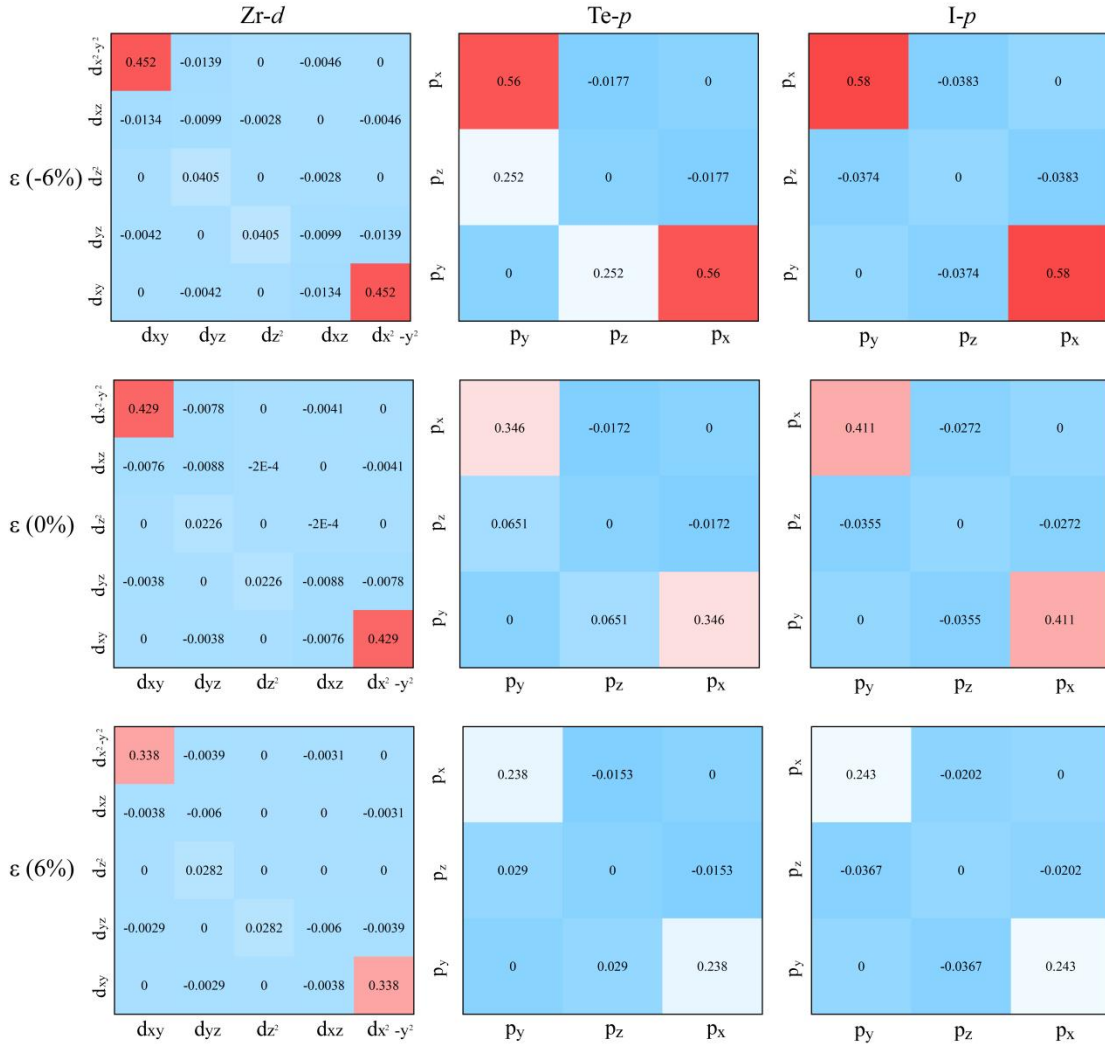


Fig. S9. Zr-d and Te/I-p orbital-resolved MCAs of Janus 2H-ZrTeI monolayers at 6%, 0% and 6% strain

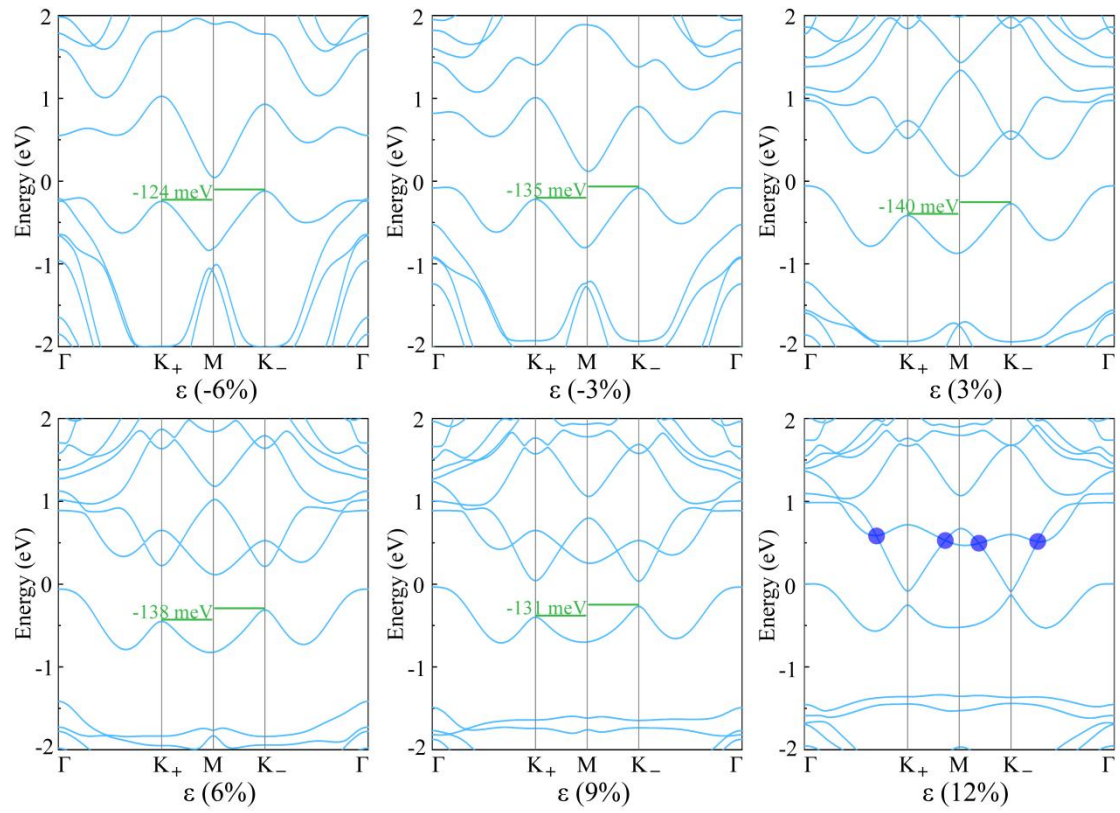


Fig. S10. Band structure of Janus 2H-ZrTeI monolayers at -6% to 12% strain.

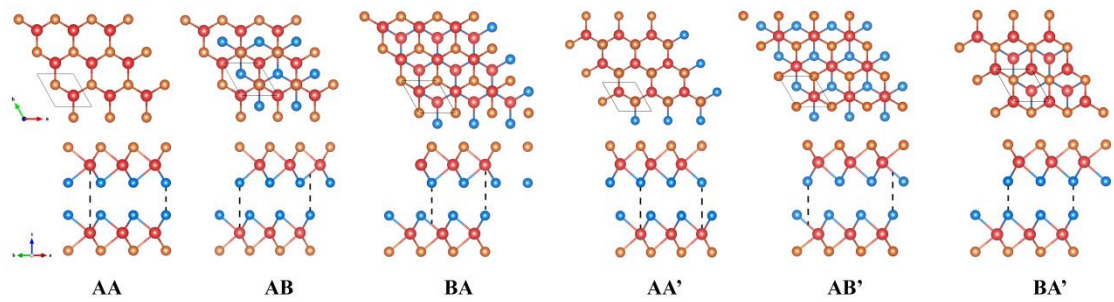


Fig. S11. Stacking structures of bilayer ZrTeI.

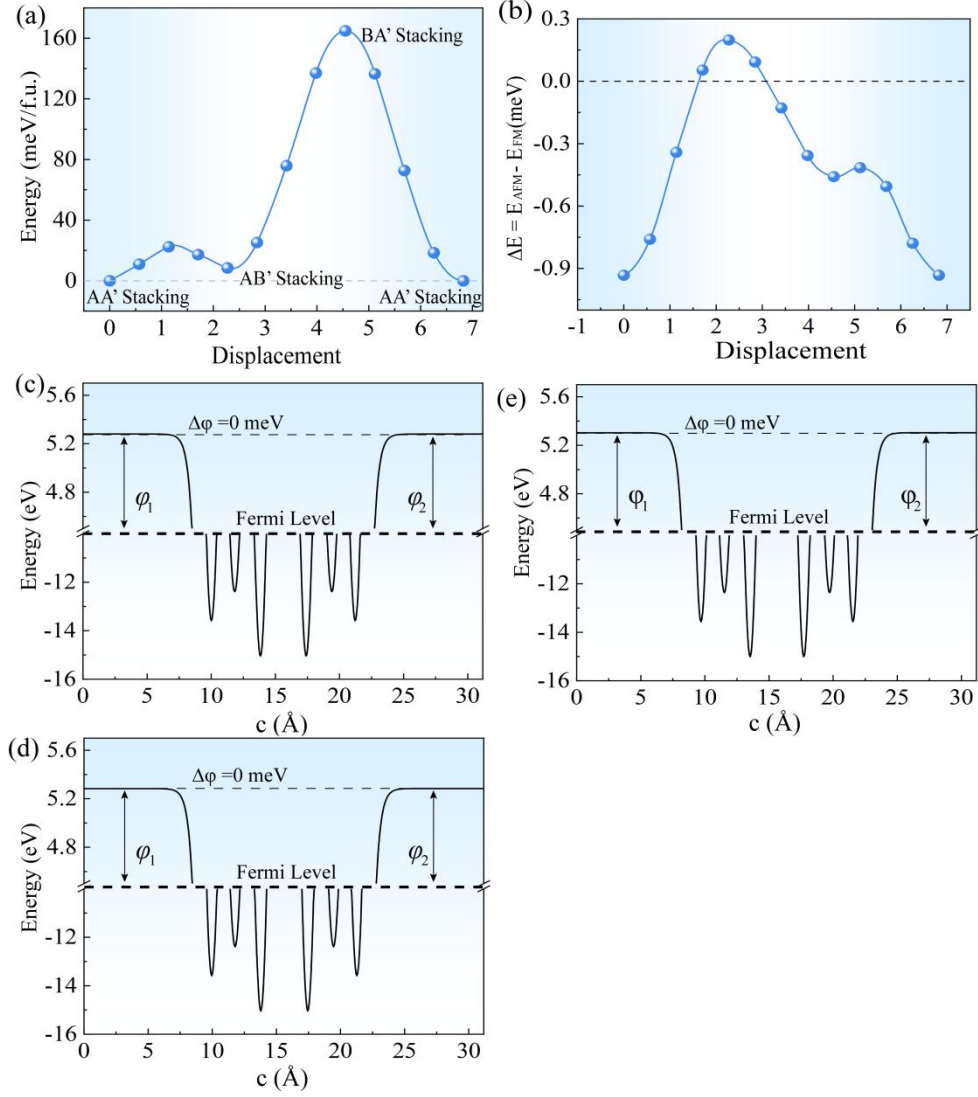


Fig. S12. (a) The sliding energy barrier between the upper and lower layers of bilayer ZrTeI. (b) The energy difference between interlayer AFM and FM states in AA' bilayer ZrTeI as a function of interlayer translation. (c) AA', (d) AB', and (e) BA' stacked bilayer ZrTeI planar-averaged electrostatic potential along the z direction.

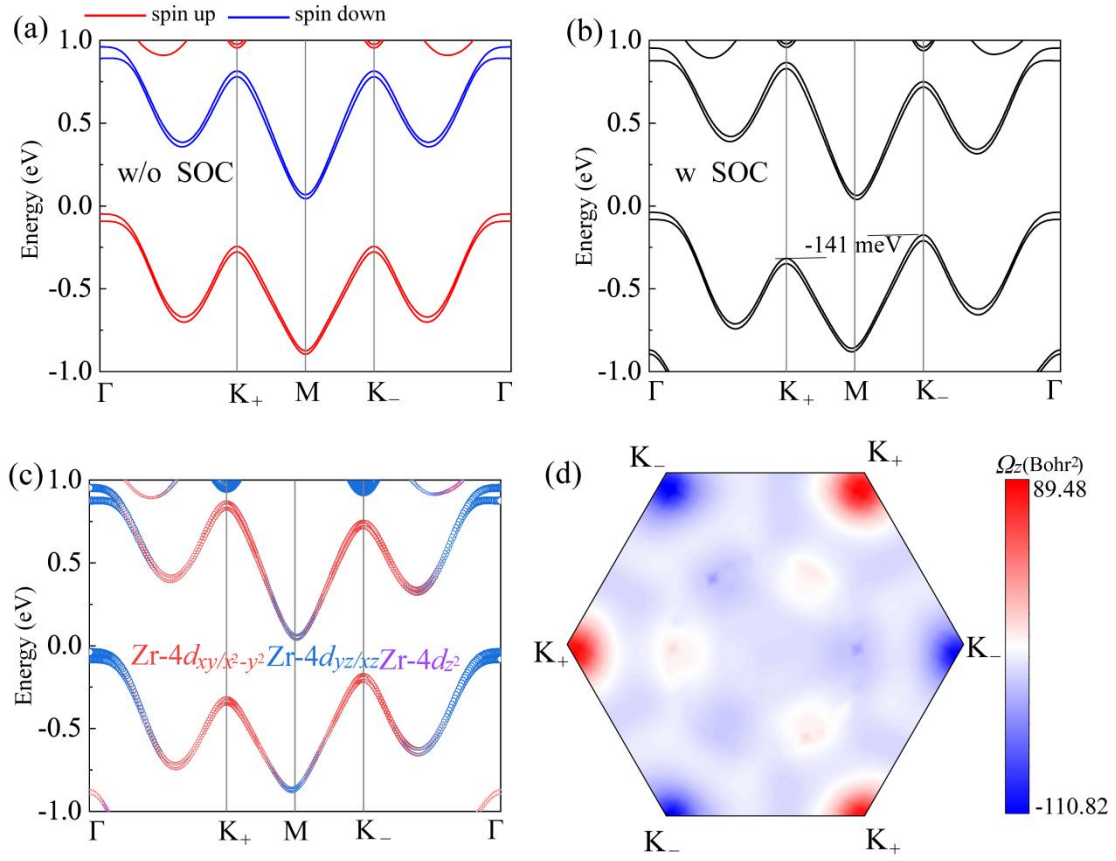


Fig. S13. (a) and (b) The band structures of BA stacked bilayer ZrTeI without and with SOC, respectively. (c) and (d) The orbital-resolved band structures and Berry curvature.